Alternative polyadenylation regulates acetyl-CoA carboxylase function in peanut

Zhenying Peng (pengzhenying2005@126.com)
Shandong Academy of Agricultural Science
Shuang Yu
Xinjiang Agricultural University
Jingjing Meng
Shandong Academy of Agricultural Science
Kaihua Jia
Shandong Academy of Agricultural Science
Jialei Zhang
Shandong Academy of Agricultural Science
Xinguo Li
Shandong Academy of Agricultural Science
Wenwei Gao
Xinjiang Agricultural University
Shubo Wan
Shandong Academy of Agricultural Science

Research Article

Keywords: Peanut, Alternative polyadenylation, Polyadenylation sites, 3'-untranslated region, Acetyl-CoA carboxylase

Posted Date: June 5th, 2023

DOI: https://doi.org/10.21203/rs.3.rs-2993404/v1

Abstract

Background

Polyadenylation is an important mechanism by which mRNA molecules are terminated at their 3'-ends. Alternative polyadenylation (APA) can produce multiple transcripts from the same locus with different polyadenylation sites (PASs) and result in several 3' untranslated regions (UTRs) varying by length and composition. APA affects approximately 60–70% of eukaryotic genes, with fundamental consequences on cell proliferation, differentiation, and tumorigenesis.

Results

In this study, we performed long-read, single-molecule sequencing of mRNA from peanut seeds, which revealed that more than half of all peanut genes have more than two PASs, with more PASs in older developing seeds, indicating that the PAS is highly tissue specific and plays an important role in peanut seed maturation. We identified four 3' UTRs for the peanut *acetyl-CoA carboxylase A1* (*AhACCA1*) gene, designated UTR1–4. RT-PCR analysis showed that UTR1-containing transcripts are expressed mainly in roots, leaves, and early developing seeds; transcripts with UTR2/3 accumulated mainly in roots, flowers, seeds; and transcripts harboring UTR4 were constitutively expressed. We transiently expressed all four UTRs in *Nicotiana benthamiana* leaves, which indicated that each UTR affects protein abundance but not subcellular location. We also transformed yeast cells with each UTR for functional verification. UTR2 promoted the expression level of *AhACCA1* compared to a yeast transcription terminator, whereas UTR3 did not. We determined *ACC* gene structures from seven plant species, detecting 51 PASs for 15 *ACC* genes from four plant species, indicating that APA of the *ACC* gene family is universal in plants.

Conclusion

Our data reveal that APA is universal in peanut seeds and plays important role in peanut seed maturation. We identified four 3' UTRs for *AhACCA1* gene, each of them showed different tissue-specific expression pattern. Using subcellular location experiment and yeast transformation test, we identified that UTR2 had a stronger effect in gene expression than the other three ones.

Background

In eukaryotes, polyadenylation is a mechanism by which mRNA molecules are terminated at their 3' ends. These added polyadenylated (polyA) tails protect mRNA from exonuclease attack and are important for transcription termination, mRNA export from the nucleus, and translation. A particular type of polyadenylation is called alternative polyadenylation (APA), when a locus can produce multiple transcripts with different polyadenylation sites (PASs) during transcription. The 3' untranslated region (UTR) plays an important role in plant differentiation and development through changes in overall protein

length and diversity induced by APA of the encoding transcripts. Almost all eukaryotic mRNAs terminate transcription by processing the 3' end of the pre-mRNA during splicing and polyadenylation. Thus, splicing and PAS determine transcript length. Genomic studies have shown that more than half of all human genes are transcribed as a suite of pre-mRNAs with distinct PASs, resulting in different 3' termini and thus producing a diverse transcriptome and proteome.

APA can be divided into two classes: (1) untranslated region APA (UTR-APA), which results in 3' UTR shortening without changing the coding region; and (2) coding region APA (CR-APA), which produces different protein isoforms through the usage of PASs residing in an intron [1]. In Arabidopsis, about 83% is UTR-APA and the remaining 17% is CR-APA [2]. The composition and length of the 3' end of different transcript isomers can change without affecting the encoded protein sequence [3, 4]. Genes with high expression levels tend to contain shorter 3' UTRs, while genes with low expression levels tend to carry longer 3' UTRs, suggesting that transcription may influence PAS selection. APA selection usually depends on the strength of sequence elements marking PAS, with long UTR sequences usually containing classical sequence motifs such as AAUAAA [5]. Shorter 3' UTRs can allow mRNAs to evade microRNA (miRNA) repression by removing the miRNA target site [6, 7]. In mouse (*Mus musculus*), shorter 3' UTRs produced by APA improve transcript stability, possibly due to the presence of fewer miRNA target sites [6]. In addition, different 3' UTRs may produce different sequences, and long UTRs may form secondary stem loop structures, which can also affect mRNA stability [8]. Studies have shown that short 3' UTRs can improve the translation efficiency of specific mRNAs [9]. Differences in the size of the 3' UTR can change the location of neuronal mRNA [10].

APA occurs in approximately 70% of all human genes, modulating gene expression by regulating 3' UTR length. This regulation affects the stability and translation efficiency of target mRNA and the cellular localization of the resulting translated proteins, fundamentally influencing various cellular programs such as proliferation, differentiation, and tumorigenesis. Recently, Li et al. constructed a multi-tissue atlas of human 3' UTR-APA quantitative trait loci (3'aQTLs), which contains about 400,000 common genetic variants associated with APA at target genes. These 3'aQTLs are largely distinct from other QTLs such as expression QTLs, with 3'aQTLs contributing substantially to the molecular mechanisms underlying human complex traits and diseases [11]. APA is involved in the regulation of many important aspects of plant biology and physiology, such as flowering, leaf development, pollen development, the circadian clock, and biotic and abiotic stresses. Yu et al. reported that over 60% of genes expressed in leaves undergo APA, with a lower extent of APA in younger leaves, but with > 70% of PAS usages changing between the second true leaf relative to cotyledons [12]. Biotic and abiotic stresses can also induce APA to produce different transcript subtypes. Under salt stress, the proportion of genes displaying APA is significantly increased in Arabidopsis (*Arabidopsis thaliana*) relative to plants grown in control conditions, but not in saltwater cress (*Eutrema salsugineum*), indicating that Arabidopsis is more sensitive to salt stress [13]. Hypoxia can produce transcripts with more PAS in the coding region [14]. Exposure to heat induced significantly more antisense PASs compared to exposure to cold and control conditions, and a unique cis-element (AAAAAA) was predominately enriched downstream of PASs in *Populus trichocarpa* genes, which was only absent in shifted PASs under the heat condition, indicating a

distinct APA mechanism responsive to heat tolerance [15]. Alternative splicing (AS) and APA were shown to regulate tissue senescence and dormancy of the fungus *Fusarium graminis* [16].

High-throughput sequencing technologies are making it easier to explore the full complement of transcripts in a cell. In particular, long-read sequencing is becoming more common. Oxford Nanopore Technology (ONT) is a typical representative of long-read sequencing that significantly improves sequence read length over previous sequencing platforms based on short reads [17, 18]. Using high-throughput sequencing, more than 50% of all genes in eukaryotes have been shown to contain more than two PASs [3]. Many loci undergoing APA have been identified and have been the focus of follow-up studies to decipher the biological effects of the resulting APA transcripts in specific tissues or at different developmental stages [19]. However, little is known about the potential role of APA in the regulation of fatty acid biosynthesis.

In this study, we performed ONT sequencing on peanut (*Arachis hypogaea* L.) seeds and determined the complement of genes whose transcripts show APA. We cloned one of these genes, *ACETYL-COA CARBOXYLASE* (*ACC*), encoding the key enzyme in plant fatty acid (FA) biosynthesis, and identified multiple 3' UTRs. The accumulation pattern of these transcripts with different 3' UTRs varied among different organs and seed development stages. Based on functional assays in budding yeast (*Saccharomyces cerevisiae*), we propose a differential role for APA in FA.

Results

ONT data collection and analysis

We divided the development of peanut seeds into four stages, designated S1 to S4 (Fig. 1A). We extracted total RNA from seeds at each stage and mixed equal amounts of total RNAs from seeds at the S1 and S2 stages, yielding the Seed 1 sample, and equal amounts of total RNAs from seeds at the S3 and S4 stages to obtain the Seed 2 sample. We generated sequencing libraries for Seed 1 and Seed 2 samples, followed by ONT sequencing. After removing short sequences and low-quality reads from the raw data, we obtained 15.28 GB of clean, high-quality reads (Table S1). We identified full-length coding sequences based on the presence of primers at both ends, corresponding to 4,836,060 and 5,173,250 clean reads for Seed 1 and Seed 2, respectively (Table S2). We obtained consensus isoform sequences by polishing each full-length sequence. We then collapsed all redundant sequences after alignment to the peanut reference genome using minimap2 software, yielding 48,435 non-redundant transcripts, representing 86.8%–87.7% of full-length sequences (Table S2).

To understand the differences at the transcriptional level, we compared the two ONT transcriptomes of Seed1 and Seed2 and found that 57 genes were significantly differentially expressed between them. Of these, 35 genes were upregulated and 22 genes were downregulated in Seed1 compared to Seed2 (Fig 1B). Heatmap analysis further confirmed these results (Fig 1C). We investigated the DEGs in more detail by subjecting the DEGs to GO term enrichment analysis and KEGG pathway enrichment analysis and results as shown in Fig. 1D-E. GO term enrichment analysis showed that the DEGs were assigned to three

GO categories: biological process, cellular component and molecular function (Fig 1D). In the “biological process” category, the genes were concentrated within the groups ‘metabolic processes’, ‘cellular process’ and ‘single-organism process’, etc. In the “cellular component” category, the predominant groups were ‘cell’, ‘cell part’, ‘organelle’ and ‘membrane’ et al. In the ‘molecular function’ category, the genes were distributed in the group of ‘catalytic activity’, ‘binding’, ‘transporter activity’ and ‘structural molecule activity’, etc. The KEGG pathways included ribosome, carbon fixation in photosynthetic organisms, phagosome and glycolysis/gluconeogenesis et al. (Fig 1E).

We looked for PASs in the two seed samples separately. More than half of all expressed genes produced transcripts with at least two PASs: 8,876 in Seed 1 and 25,081 in Seed 2, which is about 13.22% and 37.37% of all genes in the tetraploid peanut genome (usually only about half of the genes are expressed in a tissue), indicating the universality of PASs in peanut seeds (Fig 2A). Notably, Seed 2 was associated with more PAS events than Seed 1. We identified 587 genes with Seed 1–specific PAS events compared to 16,792 Seed 2–specific genes with PAS events, in addition to 8,289 genes shared by the two samples (Figure 2B, Table S3-4). This result highlights the developmental specificity of PASs. We assessed nucleotide composition over a 100-bp window centered on the PAS and detected a clear sequence bias upstream and downstream of the PAS (Figure 2C), suggesting that the identified polyA sites are authentic. We used TAPIS [20] to analyze 50-bp sequences upstream of the polyA sites and identified 16 overrepresented motifs, such as AATAATA and TATTATTA (Figure 2D).

Amplification and structural gene analysis of UTRs of AhACCA1

Peanut is one of the most important oil crops in the world, and peanut oil is popular for its fragrant smell and unique flavor. Therefore, research is needed to better understand oil biosynthesis to improve the oil content of peanut. Accordingly, we chose acetyl-CoA carboxylase (ACC), the first key enzyme in fatty acid biosynthesis, as a target for characterization of its potential PAS events. ACC catalyzes acetyl-CoA to malonyl-CoA in plants and can improve seed oil content when overexpressed in transgenic plants [21]. In our previous study, we identified 28 *AhACC* genes in the peanut genome, consisting of 4 *ACCA*, 13 *ACCB* at most, 7 *ACCC*, 2 *ACCD*, and two homogenous *ACC* (Yu et al., 2021). We detected three *AhACC* genes with APA from our ONT sequencing dataset (Figure 3A). Arahy.70V125 is an *AhACCA* gene, arahy.H4YX61 is an *AhACCB* gene, and arahy.E1R28C is an *AhACCC gene*, which we named *AhACCA1*, *AhACCB1*, and *AhACCC1*, respectively. We performed a 3' rapid amplification of cDNA ends (3' RACE) to characterize their 3' UTRs. Agarose gel electrophoresis of the PCR amplicons showed multiple bands for each reaction, indicating that each gene likely produces multiple transcript isoforms (Figure 3B).

We excised the 3' RACE bands for *AhACCA1* from the gel and cloned the 3' RACE products following gel purification of the DNA for sequencing. We aligned the sequencing results to the peanut reference genome, which revealed the existence of four different 3' UTRs for *AhACCA1*, which we named UTR1–4. UTR1 was 489 bp in length, UTR2 was 252 bp, UTR3 was 353 bp, and UTR4 was 211 bp (Figure 3C). A comparison of UTR1–4 to the peanut genome (Figure 3D) revealed that UTR1–3 harbor a single and

identical intron, only varying in the length of the sequence downstream of the intron. By contrast, UTR4 carries no intron and was the shortest among 3' UTRs. An examination of the conserved PASs for each UTR indicated that UTR1 ends with AATAAA, UTR2 with ATTTG, UTR3 with ATTTTG, and UTR4 with TATAAA. We characterized the expression pattern of each transcript isoform containing UTR1–4 in three organs (roots, leaves, and flowers) and the four seed developmental stages (S1–S4) of peanut cultivar 'Fenghua1' by RT-PCR. We observed that transcripts with UTR1 accumulate mainly in roots and leaves in the S2 and S3 stages of seed development, while transcripts containing UTR2 or UTR3 are present mainly in roots and flowers in all four stages of seed development. Transcripts with UTR4 were present at high levels in all tissues (Figure 3E). We hypothesize that the observed differences in accumulation pattern may reflect distinct functions in peanut development.

Functional analysis of UTR1–4 in *N. benthamiana* epidermal cells

To analyze the effect of each 3' UTR on the fate of the associated transcript, we replaced the *E9* terminator in the pCAMBIA1300-35S-EGFP (enhanced green fluorescent protein) vector individually with UTR1–4 from *AhACCA1* (Figure 4A). We transiently expressed each resulting construct (named *EGFP:UTR1* to *EGFP:UTR4*) into *N. benthamiana* leaf epidermal cells using pCAMBIA1300-35S-EGFP with the *E9* terminator as the control. We successfully detected green fluorescence from all constructs with similar patterns (Figure 4B) in the nucleus, cytoplasm, and along the plasma membrane, as with the *35S:EGFP* control. However, we noticed that fluorescence intensity varied among constructs, which we quantified with ImageJ software. We determined that *N. benthamiana* epidermal cells expressing *EGFP:UTR2* emit significantly more fluorescence than the control ($p < 0.01$), while those expressing *EGFP:UTR1* and *EGFP:UTR3* showed a lower fluorescence intensity than the control ($p < 0.05$). The fluorescence intensity from *EGFP:UTR4* was comparable to that of the control (Figure 4C). Compared to *EGFP:UTR2*, the *EGFP:UTR1* and *EGFP:UTR3* constructs produced significantly less fluorescence than *EGFP:UTR2* ($p < 0.01$), while *EGFP:UTR4* emitted significantly less fluorescence than *EGFP:UTR2* ($p < 0.05$) (Figure 4C). These results indicate that the four UTRs of *AhACCA1* likely affect protein synthesis but have a minor effect on subcellular protein location.

Fatty acid composition analysis of yeast strains harboring each 3' UTR

We amplified the full-length coding sequence of *AhACCA1* from total RNA extracted from the S1 seed sample. Sanger sequencing indicated that the open reading frame (ORF) of *AhACCA1* is 2,262 bp in length. We cloned the *AhACCA1* ORF into the yeast vector pESC-URA downstream of the *Gal10* (*Galactose10*) promoter and the *CYC1* terminator from *Cytochrome C1*, yielding the plasmid pESC-URA-AhACCA1. We then replaced the *CYC1* terminator from pESC-URA-AhACCA1 individually with UTR1–4, resulting in the four plasmids URA-ACCA1:UTR1, URA-ACCA1:UTR2, URA-ACCA1:UTR3, and URA-ACCA1:UTR4 (Figure 5A). We transformed each plasmid separately into yeast strain W303 and selected transformants on synthetic defined (SD) medium lacking Ura (SD–URA) for about 3–5 days. After growing the positive transformants on liquid medium for 3-5 days, the yeast cells were collected for fatty acid content analysis by GC-MS [22].

We analyzed the fatty acid content and composition of the four sets of yeast colonies harboring the control vector expressing *AhACCA1* with the *CYC1* terminator or expressing *AhACCA1* with each of the four 3' UTRs of the gene. We detected four major fatty acids in yeast: palmitic acid (C16:0), palmitoleic acid (C16:1), stearic acid (C18:0), and oleic acid (C18:1). The C16:0, C16:1, C18:0, and C18:1 content and total FA content of *URA-ACCA1:UTR2* yeast colonies were 28.8% to 51.4% higher than yeast carrying the control plasmid pESC-URA-AhACCA1 (Figure 5B), indicating some effect of UTR2 on the abundance of AhACCA1 compared to that of the *CYC1* terminator. The fatty acid content of yeast strains harboring the *URA-ACCA1:UTR3* plasmid was not different from that of the control, indicating that UTR3 has little effect on AhACCA1 abundance in yeast. UTR2 also affected the composition of fatty acids of the transformed yeast strain, decreasing the ratio of C16:0, C18:0, and C18:1 and increasing the ratio of C16:1 (Figure 5C). This result indicates that UTR2 affects the abundance of the protein being translated from the transcript.

Widespread APA among plant ACC genes

APA plays an important role in plant growth and development. The above studies showed that APA regulates the abundance of *AhACC* transcript and translatable protein in peanut leaves, roots, and seeds. To explore whether APA is present in *ACC* genes from other species, we searched the website PlantAPAdb (http://www.bmibig.cn/plantAPAdb/), which lists APA sites from seven plant species: rice (*Oryza sativa* L. [*japonica* and *indica*]), Arabidopsis (*Arabidopsis thaliana*), *Chlamydomonas reinhardtii*, barrel clover (*Medicago truncatula*), red clover (*Trifolium pratense*), black cottonwood (*Populus trichocarpa*), and Moso bamboo (*Phyllostachys edulis*) [23]. We extracted information for 15 *ACC* genes with APA from four plant species: five in Arabidopsis, one in rice, two in *T. pratense*, and seven in *M. truncatula* (Table S5). We conclude that APA of *ACC* genes is widespread in plant species.

Cis-acting elements within UTR1–4

The 3' UTRs of transcripts mediate post-transcriptional regulation. Specifically, *cis*-elements in 3' UTRs can interact with RNA-binding proteins in sequence-specific or structure-dependent manners, enabling regulation of mRNA stability, translation, and localization. The four possible 3' UTRs of *AhACCA1* are different in length and sequence, suggesting that their *cis*-elements will be at least partially distinct. We thus analyzed the motifs in the four UTRs using TBtools software [24]. UTR1 is the longest 3' UTR and had the greatest number of motifs, followed by UTR3 and UTR2; UTR4 is the shortest 3' UTR, with the fewest motifs (Figure 6A). The types of motifs also differed among 3' UTRs. Indeed, UTR1 had the most types of motifs (about 12), while UTR2 and UTR4 showed fewer types of motifs (only 5, Figure 6B). The motifs EBOXBNNAPA, GATABOX, and MYCCONSENSUSAT were present in all four 3' UTRs, while ANAERO1CONSENSUS, ANAERO2CONSENSUS, GT1GMSCAM4, and MARTBOX only appeared in UTR1. Fewer motifs suggests less regulation by RNA-binding proteins and/or expression conditions. We speculated that the stronger translation observed for UTR2 based on EGFP fluorescence intensity in *N. benthamiana* cells and FA biosynthesis in yeast can be attributed to its short length and fewer motifs.

Discussion

Transcription goes through the stages of initiation, extension, and termination. While a strong promoter is indispensable for high-level gene expression, transcription terminators are equally important. Three prime UTRs are unique sequence structures that play an important role in the regulation of transcription and mRNA stability in eukaryotes. Indeed, more than half of all human genes have been reported to use alternative splicing and alternative polyadenylation to generate mRNA isoforms that differ only in their 3' UTRs [25]. Sanfilippo et al. generated deep 3' sequencing data from 23 developmental stages, tissues, and cell lines of the fruit fly *Drosophila melanogaster*, yielding ~ 62,000 PAS, two-thirds of which are subject to APA [26]. Lu et al. identified 11,133 genes in the fungal pathogen *Fusarium graminearum* whose transcripts are alternatively polyadenylated [16]. In Arabidopsis, over 60% of genes expressed in leaves undergo APA, with evidence for developmental stage–specific regulation [12]. In this study, we identified 8,876 in Seed 1 and 25,081 in Seed 2 with at least two PASs (Fig. 2A, Table S3-4), accounting for about 79.02% of all expressed genes (32,483 genes) in the Seed 1 and Seed 2 samples. These results indicate that genes with more PAS events are associated with specific biological responses, including metabolism and cellular programs, which provides a new insight into the regulation of genes through APA.

All APA sites are found in 3' UTRs, generating mRNA isoforms with 3' UTRs of different lengths and sequence. Studies of 3' end sequencing data from diverse tissues revealed that the location of functional PASs does not vary across cell types, but the expression levels of alternative 3' UTR isoforms are highly tissue and cell type specific [27]. Tu et al. detected 6,721 genes with APA sites in Chinese tulip tree (*Liriodendron chinense*), of which 187 showed tissue-specific expression [28]. It is challenging to study the function of specific isoforms with different 3' UTRs because the derived amino acid sequences of the proteins encoded from each transcript isoform are identical. However, the 3' UTR sequence of isoforms may contain additional genetic information to distinguish the functions of their encoded protein [29]. In peanut seeds, genes with more than two PASs showed a significant tissue-specific expression pattern. We detected more PASs in the Seed 2 sample (mature stage) than in the Seed 1 sample (young stage, Fig. 2A, B), suggesting an important role for PASs in peanut seed development and maturation. In addition, the four types of *AhACCA1* transcripts with different 3' UTRs showed tissue-specific expression patterns (Fig. 3E), hinting that the proteins encoded by each transcript isoform may exert different functions in peanut leaves and roots and during seed development.

Each 3' UTR, located at the end of the transcriptional unit, plays an important role in regulating the expression of the whole gene and contains many specific functional elements that influence the efficiency of gene expression. The first example of a 3' UTR containing specific functional elements was reported for the *c-fos* gene, which lacks the ability to transform fibroblasts in culture, while *v-fos* can. Subsequent studies have revealed that *c-fos* can transform fibroblasts when the 3' UTR is omitted, which prevented the destabilization of *c-fos* transcripts via the AU-rich elements in the 3' UTR [30, 31]. Interestingly, AU-rich elements are sometimes more conserved than the coding regions of some genes and are thought to be the recognition signal for an mRNA processing pathway that specifically degrades the mRNAs for certain genes (Kruys et al., 1989; Shaw and Kamen, 1986). In addition, AU-rich elements have been shown to increase protein production [32, 33] by recruiting specific *trans*-acting factors that

bind to the *cis*-elements within a particular 3' UTR. In this study, we identified many *cis*-elements in the 3' UTRs of *AhACCA1*, some of which (such as EBOXBNNAPA, GATABOX, and MYCCONSENSUSAT) were shared by all 3' UTRs, while some (such as ANAERO1CONSENSUS, ANAERO2CONSENSUS, GT1GMSCAM4, and MARTBOX) were specific to certain 3' UTRs (Fig. 6), which may affect the efficiency of translation or mRNA stability. Results obtained from transient expression of *EGFP* constructs in *N. benthamiana* leaf epidermal cells and stable expression in yeast cells both showed that the shorter UTR2, which contains fewer motifs than the other three 3' UTRs of *AhACCA1*, is associated with high expression level, indicating the substantial effect of length and motifs.

To maximize expression, careful selection of transcription terminators (3' UTRs) have proven to be indispensable. At present, 3' UTRs, such as those from the *Nopaline synthase* (*NOS*) or *Octopine synthase* (*OCS*) genes from Agrobacterium and the 35S terminator from cauliflower mosaic virus, are widely used in plant expression vectors [34]. Several studies have shown that plant 3' UTRs have a higher potential to increase expression compared to *NOS*, *OCS*, or 35S 3' UTRs. In alfalfa (*Medicago sativa*), tobacco (*N. tabacum*), and *N. benthamiana*, the use of the 3' UTR from *Ribulose-1,5-bisphosphate carboxylase* (*rbcS*) results in higher expression levels from reporter genes than when using the *NOS* terminator. In rice seeds, the accumulation of mite allergen (mDer f 2) was four times higher when expressed from transgenes harboring the 3' UTR of *glutelin B-1* (*GluB-1*, rice), compared to the *NOS* terminator [35]. Similarly, the 3' UTRs of *GluB-5*, *GluA-2*, and *GluC* also resulted in high levels of expression compared to the *NOS* terminator in rice [36]. Another popular 3' UTR is from the *HEAT SHOCK PROTEIN* (*HSP*) gene, conferring high expression levels to the target genes in both monocot and dicot species, compared to the *NOS*, *OCS*, or 35S terminator. Up to now, some plant 3' UTRs showed greater potential to drive high expression levels relative to the *NOS*, *OCS*, or 35S terminator, for example, the 3' UTR of *ALCOHOL DEHYDROGENASE* (*ADH*), *histone H4* (*H4*), and *UBIQUITIN 5* (*UBQ5*) [37]. In this study, we identified four 3' UTRs for the *AhACCA1* locus. Transient and stable expression assays indicated that the four 3' UTRs show different expression power, with UTR2 resulting in the highest expression level compared to the other three 3' UTRs from *AhACCA1*, as well as compared to pea *E9* (derived from *RbcS*) and the yeast *CYC1* terminator. By contrast, UTR1 and UTR3 showed a lower expression level than the control terminator (Figs. 4 and 5). Therefore, it is necessary to select a suitable transcription terminator for appropriate expression of target genes.

Many types of transcription terminators have been studied in plants, but few studies have been conducted on those derived from FA biosynthesis genes. Peanut is an important oil crop, so it is necessary to study the regulatory mechanism of its oil biosynthetic genes. The main substrate of FA biosynthesis is acetyl-CoA, which is catalyzed by ACC. Therefore, the enzyme activity of ACC has a direct influence on FA biosynthesis and oil content. Here, we discovered that *AhACCA1* possesses four 3' UTRs, each appearing to be associated with mRNA stability or translation efficiency, offering new clues about the regulation of *AhACCA1* expression. We further investigated whether *ACC* genes in other plants are subjected to APA. Indeed, we detected multiple transcripts from distinct *ACC* genes in other plants, such as Arabidopsis, rice, *T. pratense*, and *M. truncatula*, highlighting the widespread nature of APA for *ACC*

genes (Table S5). Therefore, understanding the regulatory mechanism of 3' UTRs from *AhACCA1* will be helpful to elucidate how *ACC* gene expression is regulated in peanut and other species.

Conclusions

In this study, we subjected total RNA extracted from developing peanut seeds to long-read-based ONT sequencing and identified the complement of genes with APS in peanut seeds. We tested four 3' UTRs from *AhACCA1* by RT-PCR, revealing varying expression levels in different organs for each of their corresponding cognate transcript isoforms. Transient expression of each 3' UTR cloned downstream of *EGFP* into *N. benthamiana* leaf epidermal cells and stable expression in yeast cells downstream of the *AhACCA1* coding sequence showed that each 3' UTR has a different influence on the targeted genes, with UTR2 displaying a strong ability to support high expression levels. APS appears to be widespread among *ACC* genes, rather than being specific to peanut, indicating that it is pervasive in plant fatty acid biosynthesis.

Materials and methods

ONT sequencing and data analysis

One microgram of total RNA was prepared from peanut seeds of different development stages for cDNA libraries using a cDNA-PCR Sequencing Kit (SQK-PCS109) following the protocol provided by Oxford Nanopore Technologies (ONT). Briefly, the template-switching activity of reverse transcriptase was used to enrich for full-length mRNAs. Defined PCR adapters were added directly to both ends of the first-strand cDNA, followed by amplification by PCR for 14 circles with LongAmp Tag (NEB). The PCR products were then subjected to ONT adapter ligation using T4 DNA ligase (NEB). Agencourt XP beads were used for DNA purification according to the ONT protocol. The final cDNA libraries were loaded onto a FLO-MIN109 flowcell for sequencing on a PromethION platform from Biomarker Technology Company (Beijing, China). Raw reads were filtered for a minimum average read quality score of 7 and a minimum read length of 500 bp. Ribosomal RNA was discarded after mapping to the rRNA database (http://www.peanutbase.org). Next, full-length, non-chimeric (FLNC) transcripts were determined by searching for primers at both ends of the reads. Clusters of FLNC transcripts were obtained after mapping to the peanut reference genome (http://www.peanutbase.org) with mimimap2 [38], and consensus isoforms were obtained after polishing within each cluster by pinfish. Consensus sequences were mapped to the reference genome using minimap2. Mapped reads were collapsed by the cDNA_Cupcake package with min-coverage = 85% and min-identity = 90%.

Transcripts were validated against known annotation files for peanut with gffcompare [39]. APA analysis was conducted with TAPIS [20]. Coding sequences were predicted by TransDecoder [40]. Functional gene annotation was performed based on the following databases: NR (NCBI non-redundant protein sequences), Pfam (Protein family), KOG/COG/eggNOG (Clusters of Orthologous Groups of proteins),

Swiss-Prot (A manually annotated and reviewed protein sequence database), KEGG (Kyoto Encyclopedia of Genes and Genomes), and GO (Gene Ontology).

Full-length reads were mapped to the reference transcriptome (http://www.peanutbase.org). Reads with match quality above 5 were used for quantification. Expression levels were estimated based on number of reads per gene/transcript per 10,000 reads mapped. Prior to differential gene expression analysis, for each sequenced library, the read counts were adjusted with the R package edgeR through one scaling normalized factor (Robinson et al., 2010). Differential expression analysis between two samples was performed using edgeR (3.8.6). A false discovery rate (FDR) < 0.01 and a fold-change ≥ 2 were set as the threshold for significant differential expression.

RACE amplification

Total RNA was extracted from the seeds of peanut cultivar 'Fenghua 1' with RiboPure RNA Purification Kits (ThermoFisher) and reverse transcribed into first-strand cDNA using a HiScript-TS 5'/3'RACE Kit (Vazyme Biotechnology Co., LTD, Nanjing, China) according to the manufacturer's manual.

Cloning of the AhACCA1 coding sequence

The coding sequence of *AhACCA1* was amplified by PCR using primers accA1-F and accA1-R (Table S6). Each 25-μL reaction contained 1 μL cDNA (100 ng/μL) from Seed 1, 1 μL of each primer (10 μM), 12.5 μL 2× Phanta® Max Master Mix (Dye Plus), and 9.5 μL ddH_2O. The amplification program comprised an initial denaturation (95°C for 3 min), followed by 30 cycles of 95°C for 15 s, 60°C for 15 s, and 72°C for 90 s, with a final elongation of 72°C for 5 min. The amplicons were resolved by electrophoresis on a 1% (w/v) agarose gel, gel purified with a PureLink™ PCR Purification kit (ThermoFisher), and sequenced by Sangon Biotech (Shanghai, China).

Cloning of the 3' UTRs of AhACCA1

Nested PCR was conducted to amplify the 3' UTRs of *AhACCA1* using primers UTR-1-F, UTR-2-F, and UTR-R (Table S6). The fragments were subcloned into the pCE2 TA/Blunt-Zero vector (Vazyme, Nanjing,China) for sequencing. The 3' UTRs were compared with the corresponding genomic sequence to determine gene structure using the online software GSDS 2.0 [41].

RT-PCR tests of the 3' UTRs in different tissues

Total RNAs from young roots, leaves, flowers, and the seeds of S1–S4 stages of peanut cultivar 'Fenghua 1' were isolated and reverse transcribed into first-strand cDNAs using the FastPure Plant Total RNA Isolation Kit (Vazyme Biotechnology Co., LTD, Nanjing, China) according to the manufacturer's manual. S1 seeds were swollen, with a smooth surface, a foxnut-like, white spongy tissue, and a tiny embryo. S2 seeds were about 5–6 mm in length with a white episperm and a very small inner embryo. S3 seeds were about 10 mm in length, and the embryo was not mature. S4 seeds were about 15–16 mm in length, and the embryo was fully mature. The cDNAs were diluted to the same concentration, and the peanut *Actin*

gene (Actin-F and Actin-R, Table S6) was used as the reference. Primers UTR-1-F, UTR-4-F, and UTR-R were used to amplify the fragments of 3' UTRs from different organs. Each 20-μL reaction consisted of 1 μL cDNA (100 ng/μL), 1 μL of each primer (10 μM), 10 μL 2×Taq Master Mix, and 7 μL RNase-free H_2O. The amplification program comprised an initial denaturation (95°C for 1 min), followed by 30 cycles of 95°C for 15 s, 60°C for 15 s, and 72°C for 40 s, with a final elongation of 72°C for 5 min. The amplicons were resolved by electrophoresis on a 1.2% (w/v) agarose gel.

Subcellular localization of proteins encoded by AhACCA1 transcripts

Full-length sequences of the four 3' UTRs of *AhACCA1* were amplified using primers (GFP-1-F-Sal I, GFP-1-R-Hind III, GFP-2-R-Hind III, GFP-3-R-Hind III, GFP-4-F-Sal I, and GFP-4-R-Hind III, Table S6) containing the sites for the restriction enzymes *Sal* I and *Hind* III and cloned into the pCAMBIA1300-35S-EGFP vector. The E9 terminator of EGFP was replaced to verify the functionality of the 3' UTRs. The resulting clones were named *EGFP-UTR1*, *EGFP-UTR2*, *EGFP-UTR3*, and *EGFP-UTR4* and were individually transformed into Agrobacterium (*Agrobacterium tumefaciens*) strain GV3101 according to Gui et al. [42]. The appropriate cell density of each bacterial culture was infiltrated into *Nicotiana benthamiana* epidermal cells. The plants were placed in the dark for 1 day and then in dysphotic conditions (illumination intensity: ~50 lx) for 1–2 days before peeling off the leaf abaxial epidermis for observation using a confocal microscope (Leica TCS-SP8 SR, German). An Agrobacterium suspension harboring the pCAMBIA1302-35S-EGFP empty vector was used as the control.

Yeast genetic transformation and fatty acid tests

The full-length coding sequence of *AhACCA1* was amplified using primers (URA-accA1-Xho-F I and URA-accA1-KpnI-R, Table S6) and cloned into the multiple cloning site of the pESC-URA vector by double digestion with *Xho* I and *Kpn* I. The recombinant vector was named pESC-URA-AhACCA1.

The four 3' UTRs were amplified using specific primers (URA-1-F-Kpn I, URA-1-R-BsrG I, URA-2-R-BsrG I, URA-3-R-BsrG I, URA-4-F-Kpn I, and URA-4-R-BsrG I, Table S6) and inserted into the above pESC-URA-*AhACCA1* vector by double enzyme digestion with *Kpn* I and *BsrG* I to replace the original *CYC1* terminator. The resulting clones were named URA-ACCA1-UTR1, URA-ACCA1-UTR2, URA-ACCA1-UTR3, and URA-ACCA1-UTR4. The recombinant vector pESC-URA-AhACCA1 with the *CYC1* terminator was used as control. All clones were individually transformed into yeast strain W303; positive clones were grown on galactose-induced SD–URA medium. Positive transformants were used for fatty acid tests by gas chromatography–mass spectrometry (GC-MS) according to Zheng et al. [22].

Analysis of cis-acting elements in UTR1–4

The analysis of *cis*-acting elements in UTR1–4 was performed using the online server PlantCARE [43]. The distribution of motifs in each UTR was drawn using TBtools [44].

Comparison of PASs of other plant species

The keyword “Acetyl-CoA Carboxylase” was entered on the website PlantAPAdb (http://www.bmibig.cn/plantAPAdb/) and searched in all databases. The gene structures were drawn according to the pictures shown on the website.

Declarations

Ethics approval and consent to participate

Not applicable.

Consent for publication

Not applicable.

Availability of data and materials

The datasets used and/or analysed during the current study available from the corresponding author on reasonable request. The collection and handling of plant were in accordance with all the relevant guidelines.

Competing Interest

The authors declare that they have no competing financial interests or personal relationships that could influence the work reported in this paper.

Funding

This work was supported by the National key research and development program of China (2022YFD1000105); the Shandong Province Natural Science Foundation project (ZR2020MC057); and the Shandong Provincial Key Research and Development Program/Major Scientific and Technological Innovation Project (2021LZGC025).

Author Contribution

Zhenying Peng and Shuang Yu conceived and designed the experiments. Jingjing Meng performed subcellular localization experiment. Kaihua Jia assisted in transcriptome data analysis and interpretation. Jialei Zhang performed vector construction and genetic transformation. Xinguo Li performed fatty acid composition analysis. Wenwei Gao and Shubo Wan contributed to the writing of the manuscript. All authors have read and approved the final manuscript.

Acknowledgements

Not applicable.

References

1. Giammartino DCD, Nishida K, Manley JL: **Mechanisms and Consequences of Alternative Polyadenylation**. *Molecular Cell* 2011, **43**(6):853-866.
2. Wu X, Liu M, Downie B, Liang C, Ji G, Li QQ, Hunt AG: **Genome-wide landscape of polyadenylation in Arabidopsis provides evidence for extensive alternative polyadenylation**. *Proc Natl Acad Sci* 2011, **108**(30):12533–12538.
3. Tian B, Manley JL: **Alternative polyadenylation of mRNA precursors**. *Nature Reviews Molecular Cell Biology* 2017, **18**(1):18-30.
4. Wei C, Qi J, Song Y, Fu H, Gang W, Ni T: **Alternative polyadenylation: methods, findings, and impacts**. *Genomics Proteomics & Bioinformatics* 2017, **15**(5):14.
5. Ji Z, Luo W, Li W, Hoque M, Pan Z, Zhao Y, Tian B: **Transcriptional activity regulates alternative cleavage and polyadenylation**. *Molecular Systems Biology* 2011, **7**(1):534.
6. Sandberg R, Neilson JR, Sarma A, Sharp PA, Burge CB: **Proliferating cells express mrnas with shortened 3' untranslated regions and fewer microrna target sites**. *Science* 2008, **320**(5883):1643-1647.
7. Mayr C, Bartel DP: **Widespread shortening of 3'UTRs by alternative cleavage and polyadenylation activates oncogenes in cancer cells**. *Cell* 2009, **138**(4):673-684.
8. Bernardes WS, Menossi M: **Plant 3' regulatory regions from mRNA-encoding genes and their uses to modulate expression**. *Frontiers in Plant Science* 2020, **11**:1252.
9. Chang J-W, Zhang W, Yeh H-S, Jong EPd, Jun S, Kim K-H, Bae SS, Beckman K, Hwang TH, Kim K-S *et al*: **mRNA 3'-UTR shortening is a molecular signature of mTORC1 activation**. *Nat Commun* 2015, **6**:7218.
10. Tushev G, Glock C, Heumüller M, Biever A, Jovanovic M, Schuman EM: **Alternative 3' utrs modify the localization, regulatory potential, stability, and plasticity of mrnas in neuronal compartments**. *Neuron* 2018:S0896627318302368.
11. Li L, Huang K-L, Gao Y, Cui Y, Wang G, Elrod ND, Li Y, Chen YE, Ji P, Peng F *et al*: **An atlas of alternative polyadenylation quantitative trait loci contributing to complex trait and disease heritability**. *Nature Genetics* 2021, **53**(7):994-1005.
12. Yu Z, Hong L, Li QQ: **Signatures of mRNA Alternative Polyadenylation in Arabidopsis Leaf Development**. *Front Genet* 2022, **26**(13):863253.
13. Ma H, Cai L, Lin J, Zhou K, Li QQ: **Divergence in the Regulation of the Salt Tolerant Response Between Arabidopsis thaliana and Its Halophytic Relative Eutrema salsugineum by mRNA Alternative Polyadenylation**. *Front Plant Sci* 2022, **13**:866054.
14. Lorenzo LD, Sorenson R, Bailey-Serres J, Hunt AG: **Noncanonical alternative polyadenylation contributes to gene regulation in response to hypoxia**. *the Plant Cell* 2017, **29**(6):1262-1277.
15. Yan C, Wang Y, Lyu T, Hu Z, Yin H: **Alternative Polyadenylation in Response to Temperature Stress Contributes to Gene Regulation in Populus trichocarpa**. *BMC Genomics* 2021, **22**(1):53.

16. Lu P, Chen D, Qi Z, Wang H, Chen Y, Wang Q, Jiang C, Xu J-R, Liu H: **Landscape and regulation of alternative splicing and alternative polyadenylation in a plant pathogenic fungus**. *New Phytologist* 2022, **235**(2):674-689.
17. Wang Y, Zhao Y, Bollas A, Wang Y, Au KF: **Nanopore sequencing technology, bioinformatics and applications**. *Nat Biotechnol* 2021, **39**(11):1348-1365.
18. Deamer D, Akeson M, Branton D: **Three decades of nanopore sequencing**. *Nat Biotechnol* 2016, **34**(5):518-524.
19. Xu HD, Ning BL, Mu F, Li H, Wang N: **Advances of functional consequences and regulation mechanisms of alternative cleavage and polyadenylation**. *Yi Chuan* 2021, **43**(1):4-15.
20. Abdel-Ghany SE, Hamilton M, Jacobi JL, Ngam P, Devitt N, Schilkey F, Ben-Hur A, Reddy ASN: **A survey of the sorghum transcriptome using single-molecule long reads**. *Nature Communications* 2016, **7**:11706.
21. Wang FL, Wu GT, Lang CX, Liu RH: **Influence on Brassica Seed Oil Content by Transformation with Heteromeric Acetyl-CoA Carboxylase (ACCase) Gene**. *Molecular Plant Breeding* 2017, **15**(3):920-927.
22. Zheng L, Shockey J, Bian F, Chen G, Shan L, Li XG, Wan SB, Peng ZY: **Variant Amino Acid Residues Alter the Enzyme Activity of Peanut Type 2 Diacylglycerol Acyltransferases**. *Front Plant Sci* 2017, **8**:1751.
23. Zhu S, Ye W, Ye L, Fu H, Ye C, Xiao X, Ji Y, Lin W, Ji G, Wu X: **PlantAPAdb: A Comprehensive Database for Alternative Polyadenylation Sites in Plants**. *Plant Physiol* 2020, **182**(1):228-242.
24. Chen C, Chen H, Zhang Y, Thomas HR, Xia R: **Tbtools: an integrative toolkit developed for interactive analyses of big biological data**. *Molecular Plant* 2020, **13**(8):1194-1202.
25. Lianoglou S, Garg V, Yang JL, Leslie CS, Mayr C: **Ubiquitously transcribed genes use alternative polyadenylation to achieve tissue-specific expression**. *Genes Dev* 2013, **27**:2380-2396.
26. Sanfilippo P, Wen J, Lai EC: **Landscape and evolution of tissue-specific alternative polyadenylation across Drosophila species**. *Genome Biology* 2017, **18**:229.
27. Lianoglou S, Garg V, Yang JL, Leslie CS, Mayr C: **Ubiquitously transcribed genes use alternative polyadenylation to achieve tissue-specific expression**. *Genes Dev* 2013, **27**:2380–2396.
28. Tu Z, Shen Y, Wen S, Liu H, Wei L, Li H: **A Tissue-Specific Landscape of Alternative Polyadenylation, lncRNAs, TFs, and Gene Co-expression Networks in Liriodendron chinense**. *Front Plant Sci* 2021, **12**:705321.
29. Mayr C: **What Are 3' UTRs Doing?** *Cold Spring Harbor perspectives in biology* 2019, **11**:a034728.
30. Miller AD, Curran T, Verma IM: **c-fos protein can induce cellular transformation: A novel mechanism of activation of a cellular oncogene**. *Cell* 1984, **36**:51-60.
31. Meijlink F, Curran T, Miller AD, Verma IM: **Removal of a 67-base-pair sequence in the noncoding region of protooncogene fos converts it to a transforming gene**. *Proc Natl Acad Sci* 1985, **82**:4987–4991.

32. Lindstein T, June CH, Ledbetter JA, Stella G, Thompson CB: **Regulation of lymphokine messenger RNA stability by a surface-mediated T cell activation pathway**. *Science* 1989, **244**:339–343.
33. Kontoyiannis D, Pasparakis M, Pizarro TT, Cominelli F, Kollias G: **Impaired on/off regulation of TNF biosynthesis in mice lacking TNF AU-rich elements: Implications for joint and gut-associated immunopathologies.** *Immunity* 1999, **10**:387–398.
34. Bernardes WS, Menossi M: **Plant 3' Regulatory Regions From mRNA-Encoding Genes and Their Uses to Modulate Expression**. *Front Plant Sci* 2020, **11**:1252.
35. Yang L, Wakasa Y, Kawakatsu T, Takaiwa F: **The 3'-untranslated region of rice glutelin GluB-1 affects accumulation of heterologous protein in transgenic rice**. *Biotechnol Lett* 2009, **31**:1625-1631.
36. Li W, Dai L, Chai Z, Yin Z, Qu L: **Evaluation of seed storage protein gene 3'-untranslated regions in enhancing gene expression in transgenic rice seed**. *Transgenic Research volume* 2012, **21**:545-553.
37. Nagaya S, Kawamura K, Shinmyo A, Kato K: **The HSP Terminator of Arabidopsis thaliana Increases Gene Expression in Plant Cells** *Plant and Cell Physiology* 2010, **51**(2):328-332.
38. Li H: **Minimap2: pairwise alignment for nucleotide sequences**. *Bioinformatics* 2018, **34**(18):3094–3100.
39. Pertea G, Pertea M: **GFF Utilities: GffRead and GffCompare**. *F1000Research* 2020, **9**:304.
40. Haas B, Papanicolaou A: **TransDecoder: Find Coding Regions Within Transcripts**. *Github Available online at: https://githubcom/TransDecoder/TransDecoder* 2015.
41. Hu B, Jin J, Guo A-Y, Zhang H, Luo J, Gao G: **GSDS 2.0: an upgraded gene feature visualization server**. *Bioinformatics* 2015, **31**(8):1296-1297.
42. Gui J, Zheng S, Shen J, Li L: **Grain setting defect1 (GSD1) function in rice depends on S-acylation and interacts with actin 1 (OsACT1) at its C-terminal**. *Front Plant Sci* 2015, **6**:804.
43. Lescot M, Déhais P, Thijs G, Marchal K, Moreau Y, Van de Peer Y, Rouzé P, Rombauts S: **PlantCARE, a database of plant cis-acting regulatory elements and a portal to tools for in silico analysis of promoter sequences**. *Nucleic Acids Research* 2002, **30**:325-327.
44. Chen C, Chen H, Zhang Y, Thomas HR, Frank MH, He Y, Xia R: **TBtools: An Integrative Toolkit Developed for Interactive Analyses of Big Biological Data**. *Mol Plant* 2020, **13**:1194-1202.

Figures

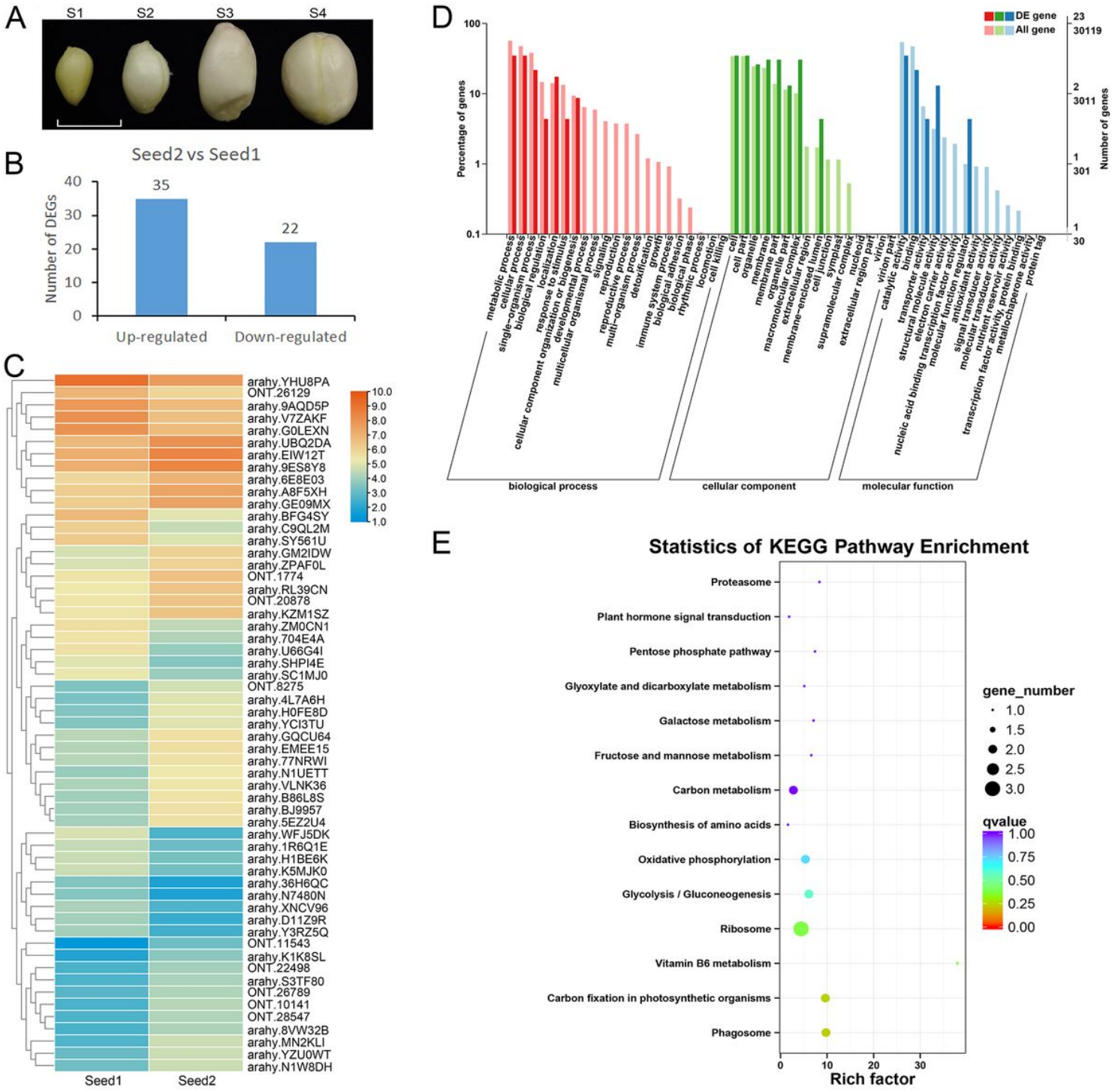

Figure 1

Long-read sequencing data analysis of transcripts from developing peanuts

A, Representative photographs of the four developmental stages of peanut seeds, S1 to S4. Scale bar, 1 cm. B, The number of upregulated and downregulated DEGs in Seed2 compared to Seed1. C, Heatmap analysis of DEGs in Seed1 and Seed2. D, GO enrichment analysis of the DEGs. F, KEGG pathways enrichment of the DEGs.

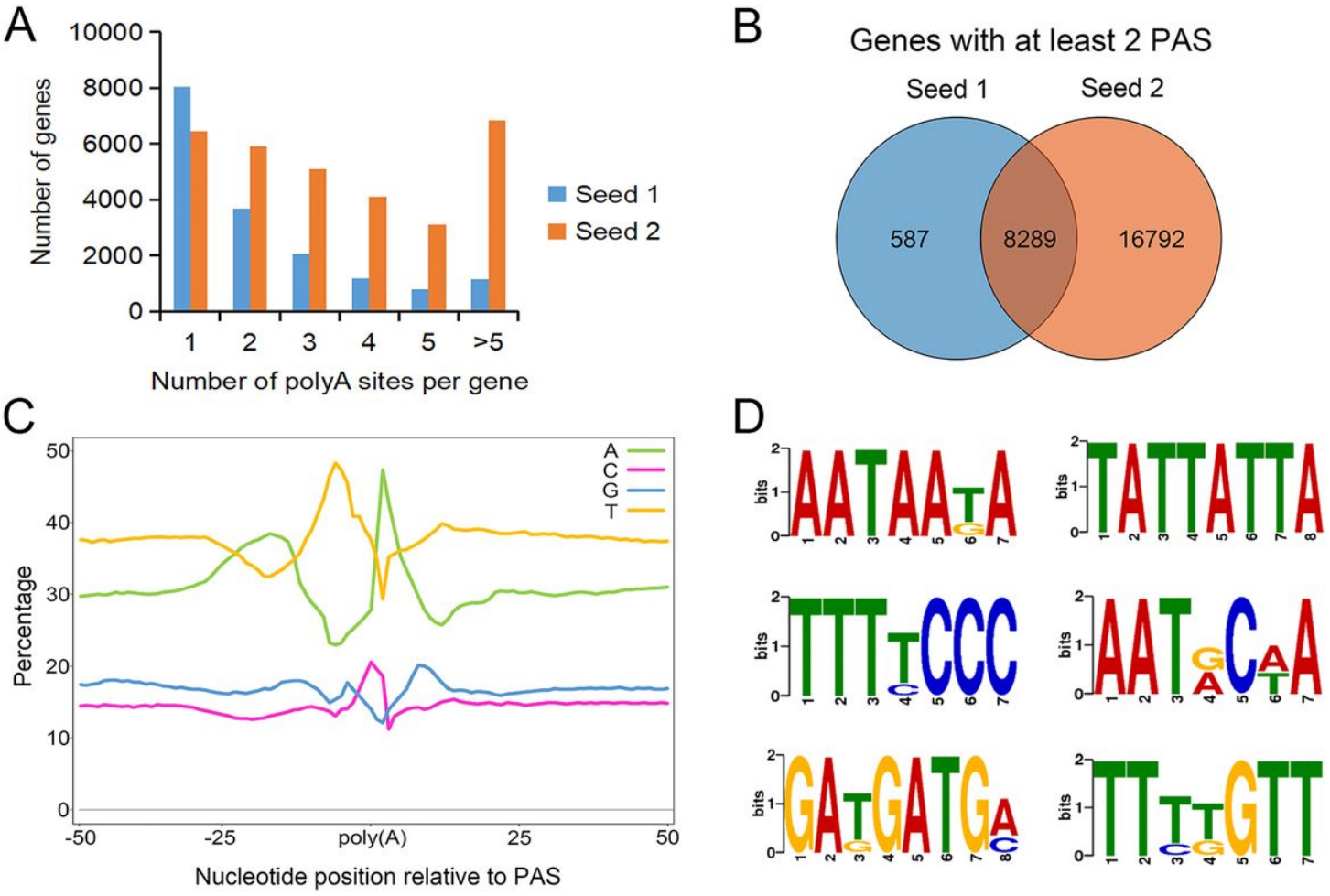

Figure 2

APA analysis of the transcripts from Seed1 and Seed2.

A, Distribution of the number of PASs per gene. Each PAS was required to be supported by at least two polyA reads, with at least 15 bp between two PAS clusters. B, Venn diagram showing the extent of overlap between the number of genes with more than two PASs in Seed 1 and Seed 2. C, Metaplot of the nucleotide composition over a 100-bp window centered around each PAS. D, Sequence logos for some of the conserved motifs distributed near the PAS.

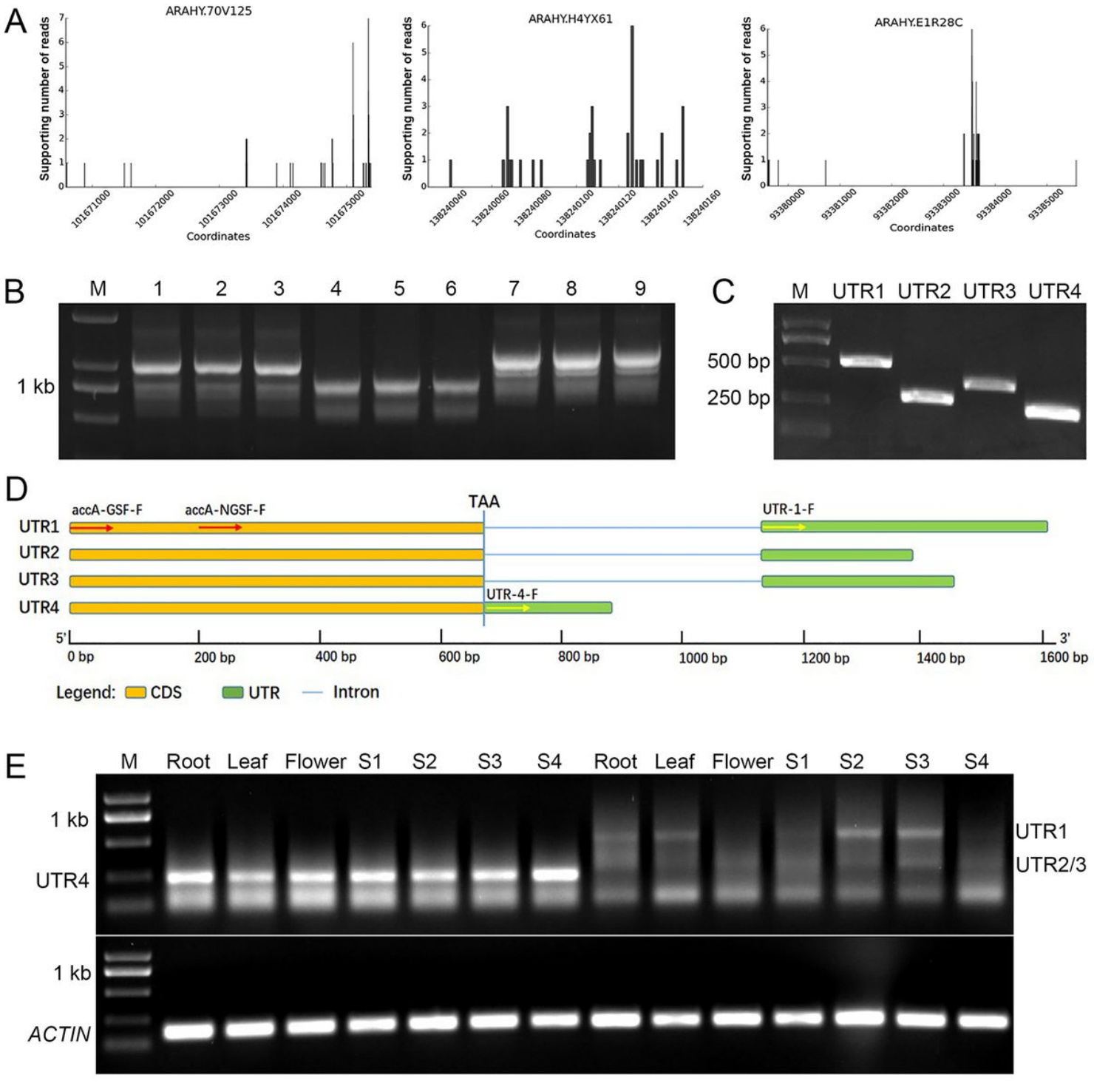

Figure 3

Molecular identification of *AhACCA1* 3' UTRs

A, *AhACCA1*, *AhACCB1*, and *AhACCC1* produce transcripts with multiple polyadenylation sites. B, 3' RACE of UTRs for *AhACCA1*, *AhACCB1*, and *AhACCC1*. C, PCR amplification of the four UTRs of *AhACCA1*. D, Schematic diagrams of the four 3' UTRs of *AhACCA1*. Red arrows indicate the forward primers of 3' RACE, and yellow arrows indicate the forward primers for amplify the UTRs sequences. E, RT-PCR

analysis of UTR1–4. M, Trans 2K plus DNA marker; S1–S4, the four different developmental stages of peanut seeds; *Actin11*, reference gene.

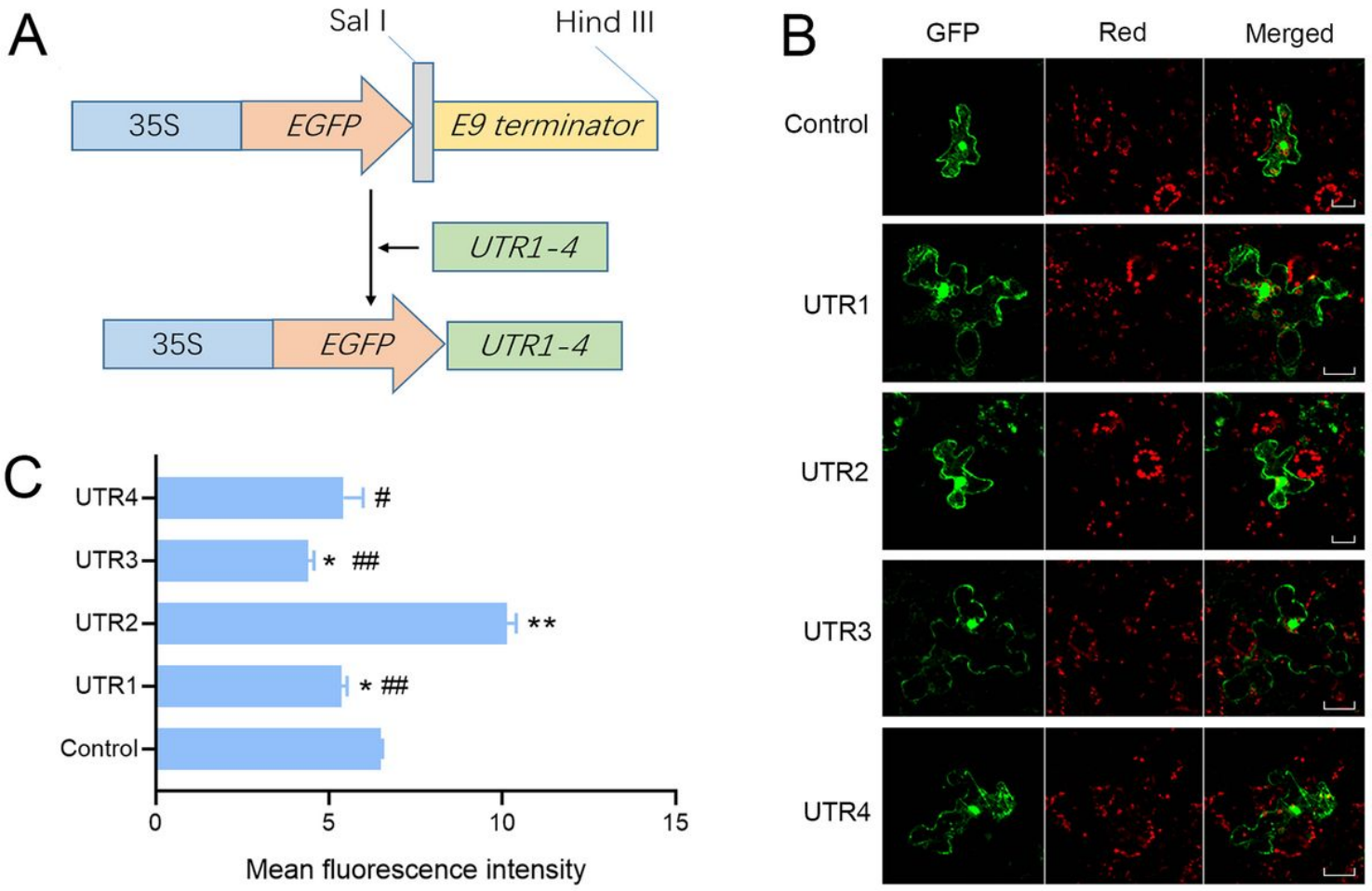

Figure 4

Effect of the 3' UTR from *AhACCA1*on protein localization and abundance in *Nicotiana benthamiana* epidermal cells

A, Schematic diagram of the constructs used to test the effect of each 3' UTR from *AhACCA1* on GFP localization. B, Representative confocal images of GFP fluorescence in *N. benthamiana* epidermal cells. Red, chlorophyll autofluorescence. Bar, 20 μm. C, Quantification of fluorescence intensity from each transformation event shown in (B). Intensity was measured with ImageJ. UTR1–4 represent *EGFP:UTR1–4*. Control is the vector harboring the *E9*terminator. Significance analysis was performed by one-way ANOVA. Asterisks represent a significant difference compared to control; # represents a significant difference compared to *EGFP:UTR2*. *, $p < 0.05$; **, $p < 0.01$; #, $p < 0.05$; ##, $p < 0.01$.

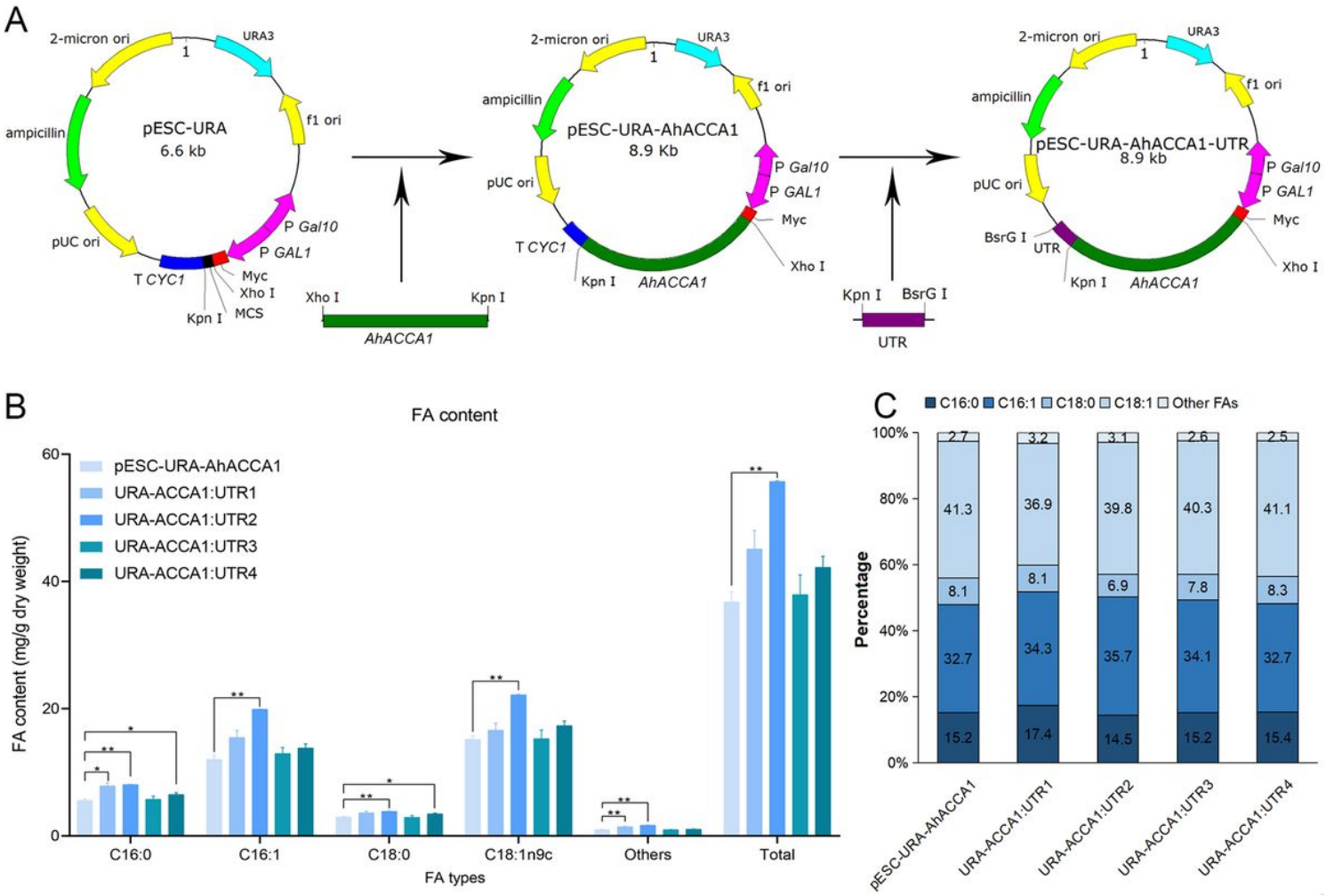

Figure 5

FA content and composition of transgenic yeast strains

A, Schematic diagram of the constructs used to test the effect of each 3' UTR from *AhACCA1* on fatty acid content in yeast. B, Mean FA content in the indicated transformed yeast colonies. C, Relative FA composition. Significance analysis was performed by two-way ANOVA. *, $p < 0.05$; **, $p < 0.01$.

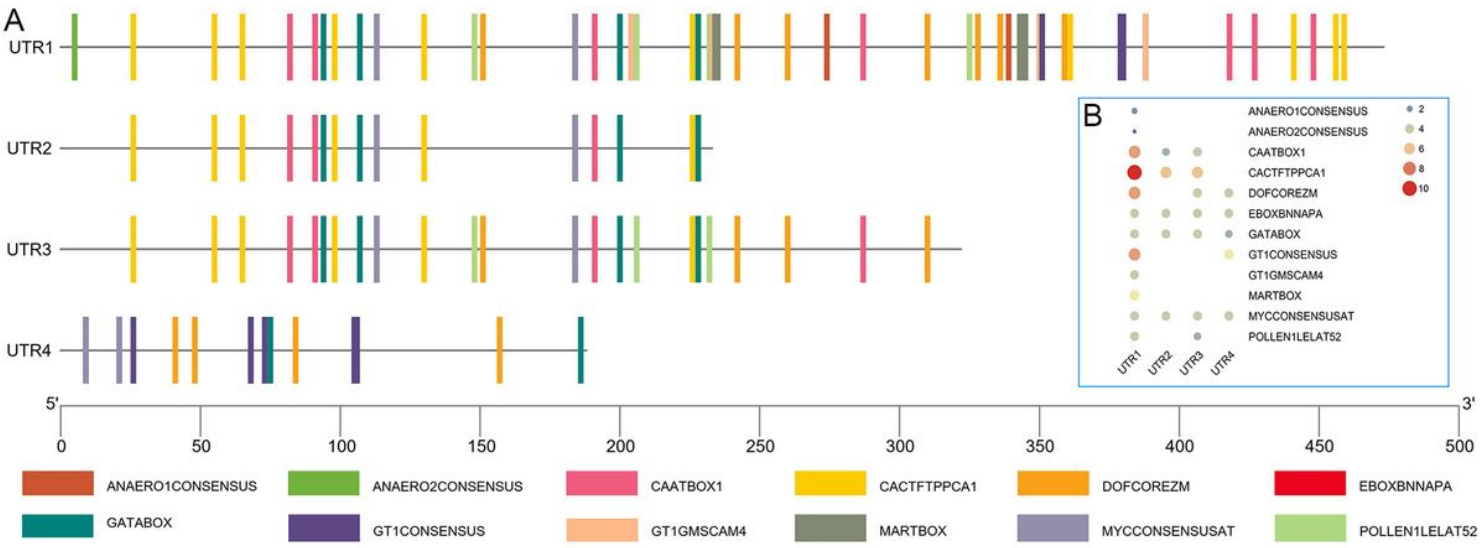

Figure 6

Cis-elements in UTR1–4 of *AhACCA1*

A, Distribution of *cis*-elements in UTR1–4. B, Number of motifs present in each 3' UTR.

Supplementary Files

This is a list of supplementary files associated with this preprint. Click to download.

- Attachmenttables.xlsx